

Physically based plasticity model coupled with precipitate model for IN718

Martin Fisk¹, Lars-Erik Lindgren²

⁽¹⁾Materials Science, Malmö University, Malmö, SE-20506, Sweden, Martin.Fisk@mah.se

⁽²⁾Dept. of Eng. Sci. and Mathematics, Luleå University of Technology, 971 87 Luleå, Sweden

Summary. This talk describes the nucleation, growth and coarsening of γ'' precipitates in Inconel 718 (IN718) during heat treatments. The model can be used in thermo-mechanical simulations of repair welding followed by heat treatment to predict residual stresses and final microstructure in aeroengine components. The interactions between precipitates and dislocations are included in a dislocation density based material model.

Key words: Strengthening mechanisms, Dislocations, Nucleation, Growth, Coarsening

Introduction

The Nickel-based superalloy IN718 is a precipitate hardening alloy commonly used in aircraft engines, power plants and gas turbines. The most important strengthening mechanism is precipitation hardening that results from around 13 vol. % of coherent ordered disk-shaped body-centred tetragonal (BCT) γ'' phase comprising nickel and niobium (Ni_3Nb). There is also a hardening contribution from ordered FCC γ' precipitates (approx. 4 vol. %). It is, however, not the dominant strengthening precipitate. The strengthening of the material depends mainly on the size of the precipitates and the volume fraction. On the other hand, the size of the precipitates depends on the ageing temperature and the time of a heat treatment.

The shape of the γ'' precipitates are disc-shaped (assumed to be oblate-shaped in the following theory) where the aspect ratio of the precipitate changes with the size of the precipitate. Due to the slightly difference in the minor and major axis for small precipitates, nucleation is assumed to follow the theory for spherical precipitates whereas the growth and coarsening follow the theory for a disc-shaped geometry. The interactions between precipitates and dislocations are included in a dislocation density based material model. Compression tests have been performed using solution annealed, fully-aged and half-aged material. Models were calibrated using data for solution annealed and fully-aged material, and validated using data from half-aged material.

Calculation of precipitate radii, nucleation rate and particle size distribution

One can distinguish three stages in a continuous precipitation process: 1) nucleation, 2) growth of the nuclei until the matrix reaches its equilibrium concentration of the solute and 3) Ostwald ripening. At least two processes may occur simultaneously, nucleation and growth or growth and coarsening (Ostwald ripening).

Nucleation and growth

The growth rate of the average precipitate depends on two components: the growth rate of existing particles of mean radius \bar{r}_p and the nucleation rate of new particles of the critical nucleation radius. Thus, we can write:

$$\left. \frac{d\bar{r}_p}{dt} \right|_{n\&g} = \left. \frac{d\bar{r}_p}{dt} \right|_g - \frac{1}{N} \frac{dN}{dt} (\bar{r}_p - r^*) \quad (1)$$

where $d\bar{r}_p/dt|_g$ is the growth rate of the average radius of existing particles, r^* is the critical nucleation radius, J_n is the homogeneous nucleation rate and N is the number of precipitates. If the nucleus is assumed to be spherical, the critical nucleation radius r^* is:

$$r^* = \frac{1}{S} \frac{2\gamma V_{at}}{kT} = \frac{R_0}{S} \quad (2)$$

where γ is the matrix/precipitate interfacial energy, S is the driving force for nucleation and V_{at} is the atomic volume. R_0 is a thermodynamic parameter that has the dimension of length. The nucleation rate depends on the surface area of the nucleus and the rate at which diffusion can occur:

$$J_0 = \frac{dN}{dt} = N_0 Z \beta^* \exp\left(-\frac{\Delta G^*}{kT}\right) \exp\left(-\frac{\tau}{t}\right) \quad (3)$$

where N_0 is the number of atoms per unit volume in the phase, Z is the Zeldovich factor (in the order of 1/20 to 1/40), $\beta^* = (4\pi r^{*2} D C_0)/a^4$ and $\tau = 1/(2\beta^* Z)$ (an incubation time). C_0 is the initial solute mole fraction, a is the lattice parameter and D is the diffusion coefficient of solute atoms in the matrix. ΔG^* is the activation energy barrier for creation of new precipitates.

The rate of change of existing spherical particles assumes to grow as if they were disk-shaped. The expression is [1]:

$$\left. \frac{d\bar{r}_p}{dt} \right|_g = \frac{2qD}{\pi} \frac{C - C_{eq}(r)}{C_p - C_{eq}(r)} \quad (4)$$

where $C_{eq}(r)$ is the equilibrium solute concentration in the matrix next to the phase boundary to a precipitate of radius r and $q = L/h$ is the aspect ratio between the major axis $L = 2r_p$ and the minor axis h of the disk respectively. The equilibrium concentration next to a precipitate of radius r is given by the Gibbs-Thomson equation. C is the current solute balance in the matrix.

Growth and coarsening

In order to achieve transformation from a metastable single-phase state to a stable two-phase state, second phase particles must first nucleate and then grow. Growth will continue until the concentration of solute is in equilibrium with the two phases. Thereafter coarsening occurs; larger precipitates will grow and smaller precipitates will disappear. In order to avoid a singularity between the two states, a linear transition is applied. During coarsening we use the LSW theory applied for disc-shape geometries [1]:

$$\left. \frac{d\bar{r}_p}{dt} \right|_c = \frac{8q}{27\pi} \frac{C_{eq}}{C_p - C_{eq}} \frac{D}{\bar{r}_p} R_0 \quad (5)$$

The corresponding rate of change in precipitate density can be written [2]:

$$\left. \frac{dN}{dt} \right|_c = \frac{1}{\bar{r}_p} \left. \frac{d\bar{r}_p}{dt} \right|_c \left[\frac{R_0 C}{\bar{r}_p (C_p - C)} \left(\frac{q}{2\pi \bar{r}_p^3} - N \right) - 3N \right] \quad (6)$$

Devaux et al. [3] gives the average aspect ratio of the γ'' precipitates, q , as a function of the precipitate radius by comparing four different sources. It is seen that the aspect ratio of the precipitates basically growth linearly where the growth rate, depending on their diameter, can be collected into two groups. The change in growth rate is correlated with the loss of coherency.

Dislocation density model accounting for precipitate hardening

Plastic deformation occurs principally by shearing the atom planes, and is facilitated by the introduction and movement of dislocations in the crystal lattice. The hardening and softening process is associated with the interaction of the material structure, which is the lattice itself, immobile dislocations, solutes, precipitates, defects etc. It is common to assume that they give contributions to the macroscopic flow stress by using expressions similar to:

$$\sigma_y = \sigma_G + \sigma^* + \sigma_p + \dots \quad (7)$$

where σ_y is the flow (yield) stress, σ_G is an athermal stress due to long-range disturbances of the lattice due to immobile dislocations, σ^* is the short-range interaction and is the stress needed to move dislocations past short-range obstacles, σ_p results from the additional stress required to move dislocations around or through precipitate and solutes. The dots tell that there may be other contributions.

The long-range term in Eq. (7) is an athermal stress contribution, which means that it is independent of temperature, i.e. thermal vibrations cannot assist dislocations in overcoming disturbances in the lattice. It is written:

$$\sigma_G = \alpha G b \sqrt{\rho_i} \quad (8)$$

where ρ_i is the effective immobile (forest) dislocation density within the microstructure of the material during deformation, b is the Burgers vector, G is the shear modulus and M is the Taylor factor. The factor α is a proportionality factor measuring the efficiency of dislocation strengthening.

The second term in Eq. (7) is the stress needed to move dislocations past short-range obstacles. It is based on the energy (Gibbs free energy) needed for a particle to overcome an obstacle taking atomic thermal vibrations into account. It can be written as [4]:

$$\sigma^* = \tau_0 G \left(1 - \left(\frac{kT}{\Delta f_0 G b^3} \ln \left(\frac{\dot{\epsilon}_{ref}}{\dot{\epsilon}^p} \right) \right)^{1/q} \right)^{1/p} \quad (9)$$

where the quantity τ_0 is depending on the strength of the obstacle (dimensionless), Δf_0 is a calibration constant, $\dot{\epsilon}_{ref}$ is a reference strain rate and p and q are calibration constants. The conditions for the exponents can be found in Lindgren et al. [4].

The last term in Eq. (7) describes the flow stress contribution due to precipitates. Precipitates, or second-phase particles, commonly act as geometric barriers to dislocation glide. If all the particles are sheared, it is possible to model the strengthening contribution as [2]:

$$\sigma_{shear} \propto \sqrt{f_p} \quad (10)$$

where G is shear modulus and f_p is the particle volume fraction. For large precipitates, it is assumed that dislocations bow around rather than shear through the particles. Ignoring the strain hardening, the stress contribution due to bowing can be modelled as [2]:

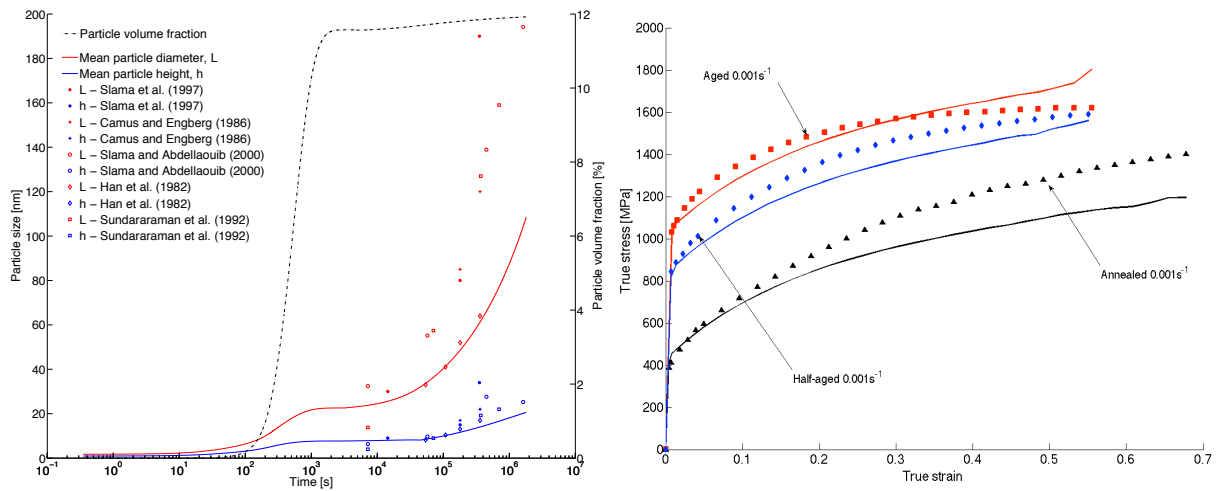
$$\sigma_{bow} \propto \frac{\sqrt{f_p}}{\bar{r}_p} \quad (11)$$

Results

The relation between the precipitate size and the addition of strengthening described earlier makes it possible to calculate the yield stress for different ageing times. This - the dislocation density model accounting for precipitate hardening and the nucleation growth and coarsening - can be applied in an incremental fashion, which is applicable in a finite element code. The

model consists of relations that describe the precipitate evolution needed in the dislocation density model according to the summary given in the previous section. The model is calibrated using compression test data at 400 °C and 600 °C for two strain rates and two states; fully-aged and solution annealed.

Figure a) shows the computational results of the particle diameter, L , height, h , and volume fraction, f_p . The results from the precipitate evolution are compared with experiments taken from journal articles. All experiments are carried out at a temperature of 750 °C. Figure b) shows measured (smoothed) and computed stress strain curves for fully-aged (heat treated for 5 h at 760 °C), half-age (heat treated for 30 min at 760 °C) and solution annealed IN718 material. The line correspond to calculated values and the symbols are measured values.



(a) Evolution of particle diameter, particle height and particle volume fraction. Computational results (full line) are compared with experiments (marks).

(b) Computed stress strain curves at 600 °C.

Conclusions

In this work, it is shown that a dislocation density based flow stress model can account for precipitate hardening. Considering the simplifications that are necessary, the material model shows good agreement with experimental measurements and is expected to be fit for its purpose; thermo-mechanical simulation of the ageing process in IN718.

References

- [1] J. Boyd and R. Nicholson. The coarsening behaviour of θ'' and θ' precipitates in two al-cu alloys. *Acta Metallurgica*, 19(12):1379 – 1391, 1971.
- [2] A. Deschamps and Y. Brechet. Influence of predeformation and ageing of an al-zn-mg alloy- ii. modeling of precipitation kinetics and yield stress. *Acta Materialia*, 47(1):293–305, 1998.
- [3] A. Devaux, L. Nazé, R. Molins, A. Pineau, A. Organista, J. Guédou, J. Uginet, and P. Héritier. Gamma double prime precipitation kinetic in alloy 718. *Materials Science and Engineering: A*, 486(1-2):117 – 122, 2008.
- [4] L.-E. Lindgren, K. Domkin, and S. Hansson. Dislocations, vacancies and solute diffusion in physical based plasticity model for aisi 316l. *Mechanics of Materials*, 40(11):907–919, 2008.